~~[illegible]~~ Declassified as per letter to W. Hoy. Jan 17, 1966

DECLASSIFIED

[redacted]

BEHAVIOR OF A CANTILEVER PLATE SUBJECTED TO RAPID EDGE HEATING

By

Louis Frederick Vosteen

Thesis submitted to the Graduate Faculty of the

Virginia Polytechnic Institute

in candidacy for the degree of

MASTER OF SCIENCE

in

Applied Mechanics

May 10, 1965

APR 1971
RECEIVED
NASA STI FACILITY
INPUT BRANCH

FACILITY FORM 602

N71 72273 (ACCESSION NUMBER) (THRU)

67 (PAGES) none (CODE)

TMX-67056 (NASA CR OR TMX OR AD NUMBER) (CATEGORY)

DECLASSIFIED

DECLASSIFIED

CONFIDENTIAL

BEHAVIOR OF A CANTILEVER PLATE SUBJECTED TO RAPID EDGE HEATING

by

Louis Frederick Vosteen

Thesis submitted to the Graduate Faculty of the

Virginia Polytechnic Institute

in candidacy for the degree of

MASTER OF SCIENCE

in

Applied Mechanics

APPROVED: APPROVED:

Director of Graduate Studies

Head of Department

Dean of Engineering

Thesis Advisor

May 10, 1955

Blacksburg, Virginia

CONFIDENTIAL

DECLASSIFIED

TABLE OF CONTENTS

CHAPTER		PAGE
I.	LIST OF FIGURES AND TABLES	3
II.	INTRODUCTION	5
III.	TEST PROCEDURE AND RESULTS	8
	A. Deformations	14
	B. Natural Frequencies	17
IV.	COMPARISON OF THEORETICAL CALCULATIONS WITH EXPERIMENTAL RESULTS	21
	A. Deformation	21
	B. Natural Frequency	21
V.	CONCLUDING REMARKS	26
VI.	ACKNOWLEDGEMENTS	27
VII.	REFERENCES	28
VIII.	VITA	29
IX.	APPENDIX	30
	A. Temperature Distribution	32
	B. Thermal Stresses	34
	C. Effect of temperature Gradient on Deflections and Natural Frequencies	43

I. LIST OF FIGURES AND TABLES

FIGURE PAGE

1. Chordwise Temperature Distribution in an Aerodynamically Heated Airfoil (ref. 1, fig. 11). 7
2. Sketch of Cantilever Plate Test Setup 9
3. Instrumentation of Test Specimen 11
4. Measured Temperature Histories for an Edge and the Midchord Line 12
5. Measured Chordwise Temperature Distributions of Radiantly Heated Plate 13
6. Measured Tip-Rotation Histories for Applied Torques of 0 and 400 in-lb. 15
7. Torsional Deformation of Plate Subjected to Rapid Edge Heating 16
8. Measured Frequency Histories for the First Bending and First Torsion Modes 19
9. Comparison of Measured and Calculated Tip Rotations for an Applied Torque of 400 in-lb. 22
10. Comparison of Measured and Calculated Frequency Changes for the First Torsion Mode 23
11. Comparison of Measured and Calculated Frequency Histories for the First Torsion Mode 23

FIGURE PAGE

12. Dimensions and Coordinate System of Cantilever Plate 33

13. Comparison of Measured and Calculated Chordwise Temperature Distributions at the Time of Maximum Edge Temperature . . . 35

14. Assumed Thermal Stress Distributions in a Cantilever Plate Rapidly Heated Along the Longitudinal Edges 37

TABLE

I. Comparison of Interaction Relations 58

II. Relative Amplitude Coefficients 59

III. Deflection of Tip, x = a 60

IV. Deflection of Edge, y = b 60

II. INTRODUCTION

One of the structural problems produced by nonuniform heating is a change in the effective stiffness of a structure caused by thermal stresses. This stiffness-change phenomenon does not depend on a change in the material properties but depends on the state of stress and may occur at stress levels well below those necessary to produce buckling. A change in stiffness may also result from changes in the material properties but these effects were found to be small in comparison with the effects of the thermal stresses. Laboratory demonstrations performed at the 1953 NACA annual inspection have shown that the natural frequency of a simplified wing structure can be effectively reduced by the nonuniform temperature distribution associated with rapid heating.

The type of temperature distribution produced by the aerodynamic heating of a thin missile wing is shown in figure 1. This figure (given in ref. 1) shows the variation in temperature across the chord of a solid double-wedge airfoil immediately following a 1g acceleration to Mach number 4 at 50,000 feet. The temperatures on the surface and at the midplane are shown. Such a temperature distribution produces longitudinal compressive stresses near the leading and trailing edges and tension in the central part of the wing. The effect of these stresses is a reduction in the stiffness of the structure that may be observed as an increased deformation under load or as a reduction in

natural frequency. No quantitative data have been found, however, which relate changes in frequency, and hence effective stiffness, to temperature distribution. The project to be discussed in this paper was devised to satisfy part of this need.

DECLASSIFIED

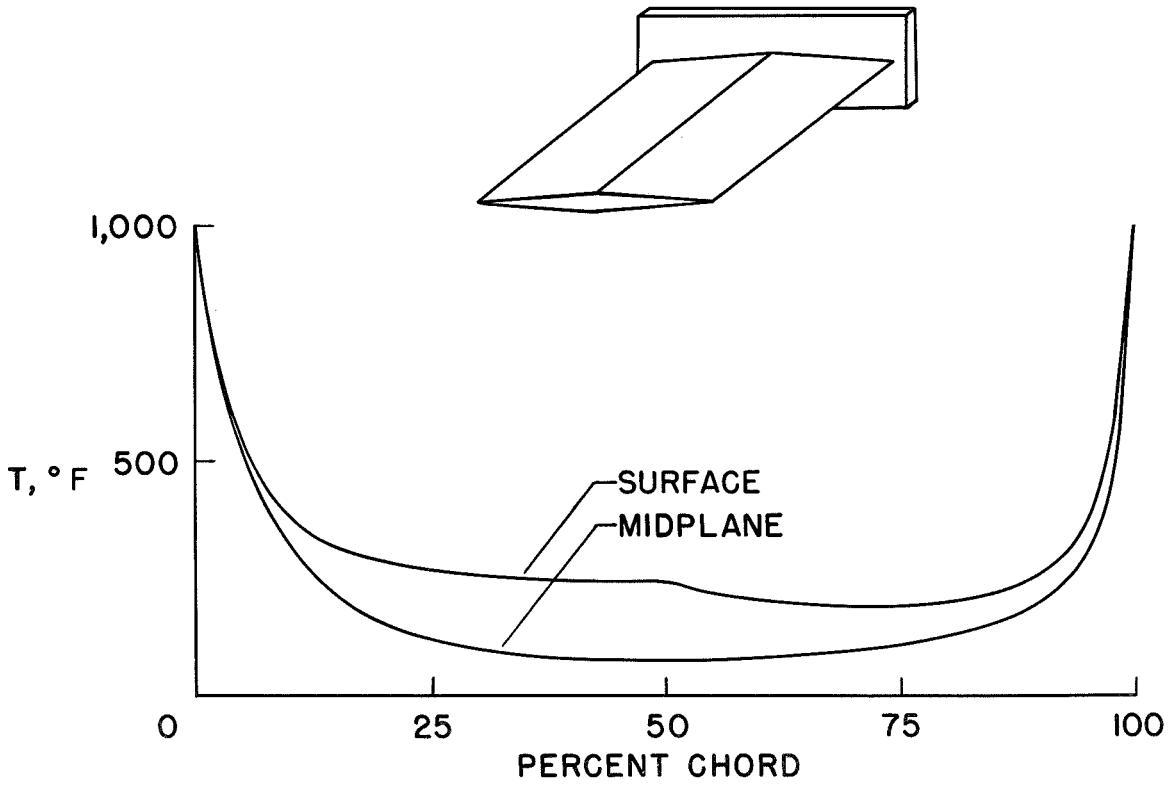

Figure 1.- Chordwise temperature distribution in an aerodynamically heated airfoil (ref. 1, fig. 11).

DECLASSIFIED

III. TEST PROCEDURE AND RESULTS

In order to investigate some of the effects of nonuniform heating experimentally, a test arrangement which resembled an aircraft wing was used. The arrangement (shown in fig. 2) utilized a thin plate of uniform thickness mounted as a cantilever. The specimen, made of 24S aluminum alloy sheet 1/4-inch thick, was 20 inches wide and 24 inches long. Four inches of the length were clamped between two 4 × 4 × 3/8 structural steel angles thus forming a clamped root and leaving a 20-inch square plate. A specimen of uniform thickness, rather than an airfoil section, was used for economy of construction and to simplify the theoretical analysis.

A nonuniform temperature distribution was produced by rapidly heating the longitudinal edges of the plate by radiation from incandescent carbon rods. The rods were heated to incandescence by passing an 800 ampere current through the rods with a voltage drop of 55 volts across each rod. The rods reached incandescence in about 5 seconds at which time a shield between the rods and the plate was removed. After the desired heating time, the shield was again interposed and the power cut off. The heated edges and 1 inch of the plate surface adjacent to the edges were painted with black lacquer to increase heat absorption.

DECLASSIFIED

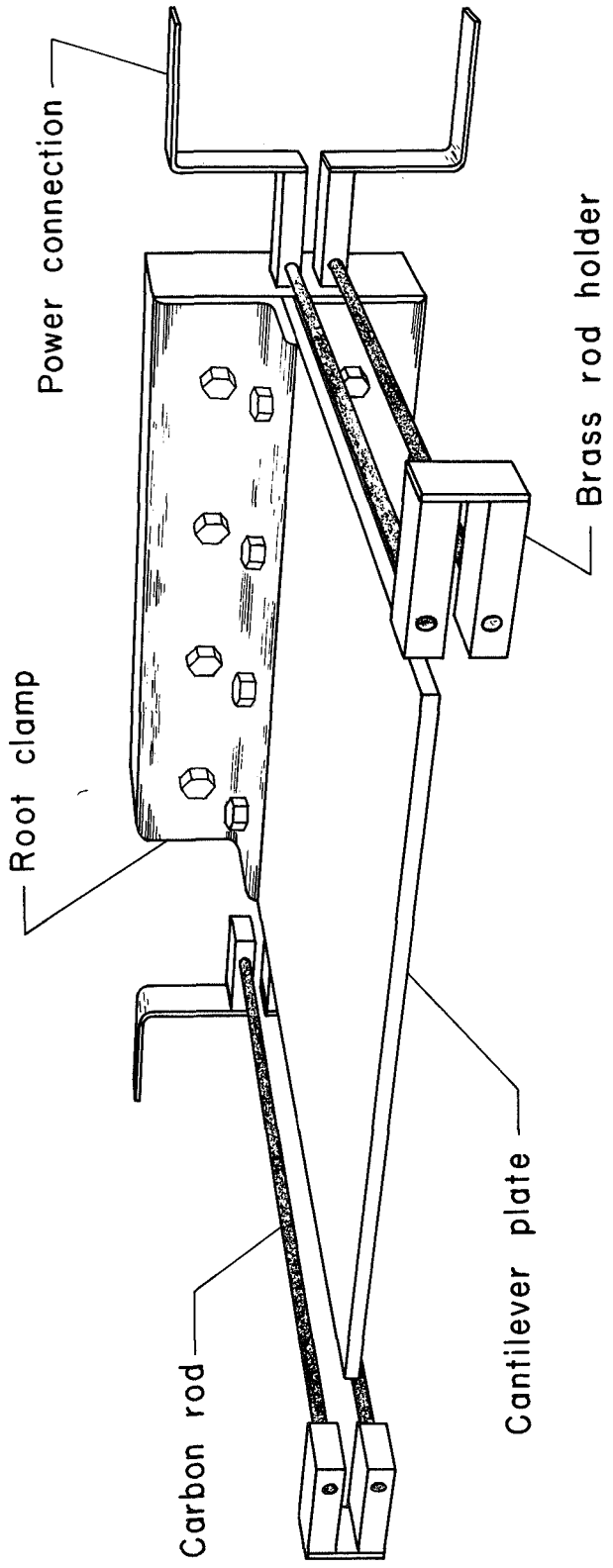

Figure 2.- Sketch of cantilever plate test setup.

DECLASSIFIED

The temperature distribution over the surface of the plate was obtained from 24 iron-constantan thermocouples which were arranged as shown in figure 3. All thermocouples, except the two on the plate edges, were peened into the surface of the plate. The two on the edges were installed about 3/64-inch from the edge at the midplane of the plate. The thermocouples were connected to Consolidated Type 5-114 recording oscillographs and temperatures were recorded continuously during the test.

The temperature distribution along the span of the plate was found to be constant except for a slight decrease toward the tip. The distribution across the chord, however, varied greatly. In figure 4 the temperature in degrees Fahrenheit of an edge and the midchord line is plotted against time in seconds. Heat is applied to the plate for about 16 seconds. During this time, the edge temperature rises almost linearly to 315° F at the peak of the heating cycle. When the heating stops, the edge temperature drops quickly and slowly levels off as the plate cools. The variation in temperature across the chord is shown in figure 5 for a time in the heating cycle (10 seconds), at the time of maximum edge temperature (16.5 seconds), and during cooling (30 seconds). These distributions show that the temperature remains relatively low over the center half of the plate, but rises sharply near the heated edges.

DECLASSIFIED

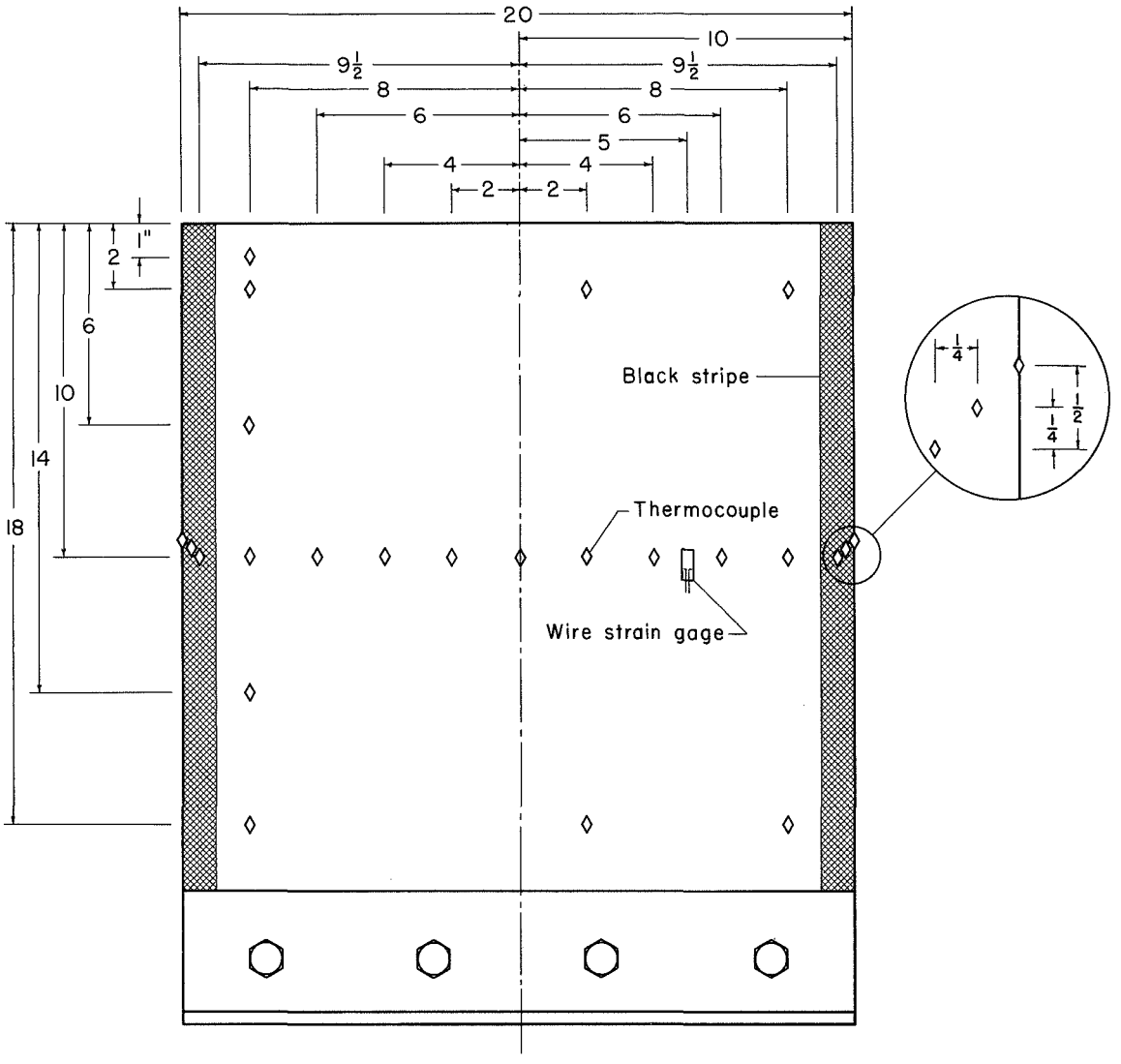

Figure 3.- Instrumentation of test specimen.

DECLASSIFIED

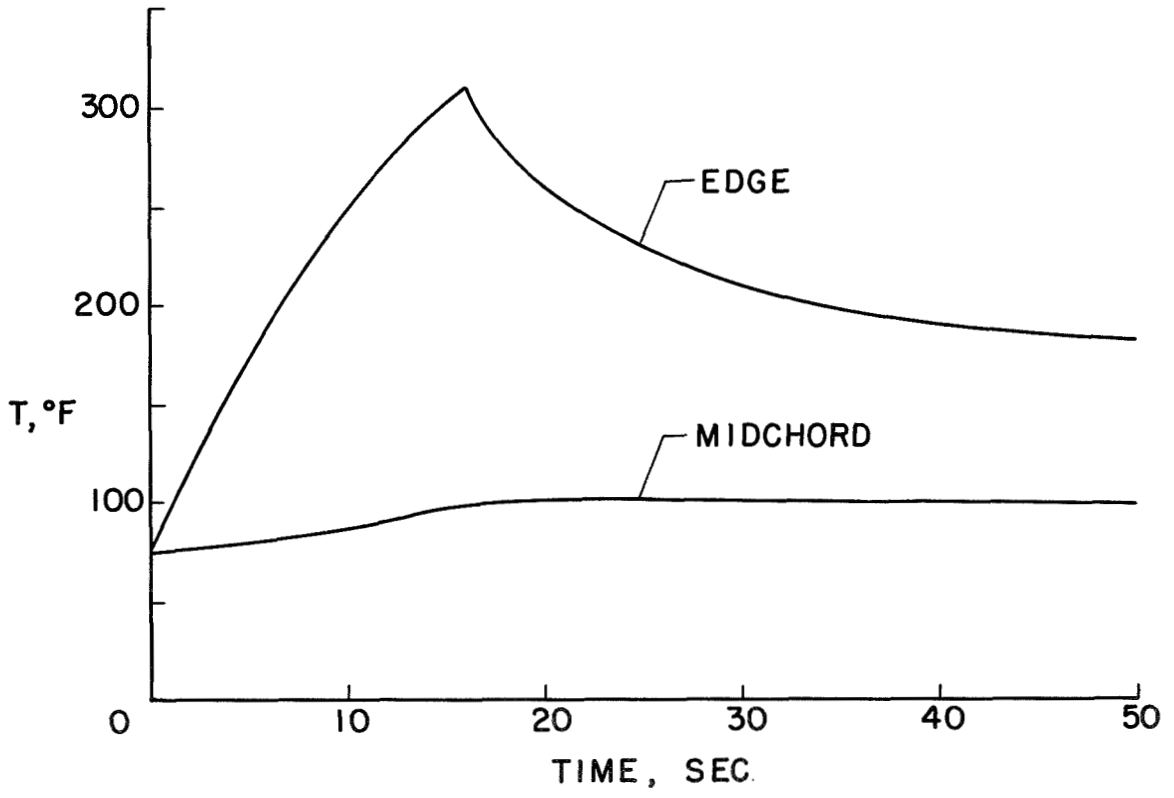

Figure 4.- Measured temperature histories for an edge and the midchord line.

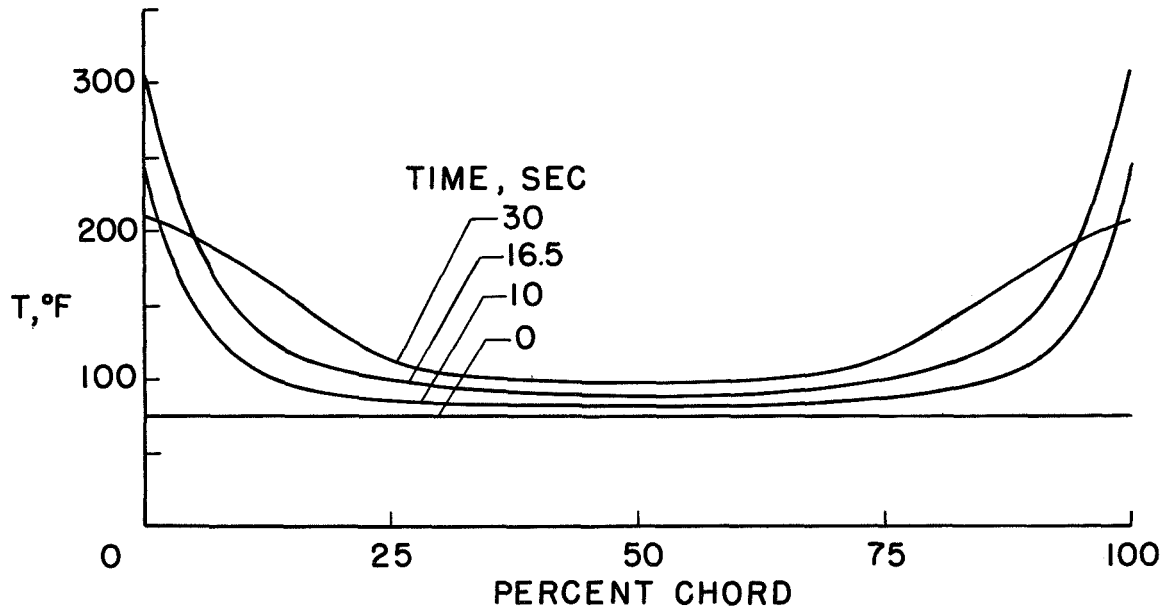

Figure 5.- Measured chordwise temperature distributions of radiantly heated plate.

DECLASSIFIED
CONFIDENTIAL

Two investigations were made to determine the effect of the nonuniform temperature distribution on the stiffness. First, the vertical deflections of the plate due to thermal stresses were obtained for various load conditions. Second, the changes in natural frequency of vibration during heating were investigated.

A. Deformations

A comparison of the plate deformations for the various load conditions was made by measuring the deflections of two points near the free corners of the plate with differential transformer gages. The output from the gages was fed into the recording oscillograph through a Consolidated Type 1-113 Bridge Amplifier. The angle of rotation (in a plane perpendicular to the plane of the plate) of a line connecting these two points was calculated from the deflection data and will be called the "angle of tip rotation."

Figure 6 shows the tip-rotation histories. The angle of tip rotation in degrees is plotted against time in seconds during heating and cooling for no external load and for applied torques of 400 inch-pounds in each direction. Torques were produced by applying two equal, concentrated loads perpendicular to the plane of the plate and in opposite directions at the free corners so as to form a couple about the midchord line. In each case, the plate deformed by rotating torsionally about the midchord line in the manner shown in figure 7. As the plate

CONFIDENTIAL

DECLASSIFIED

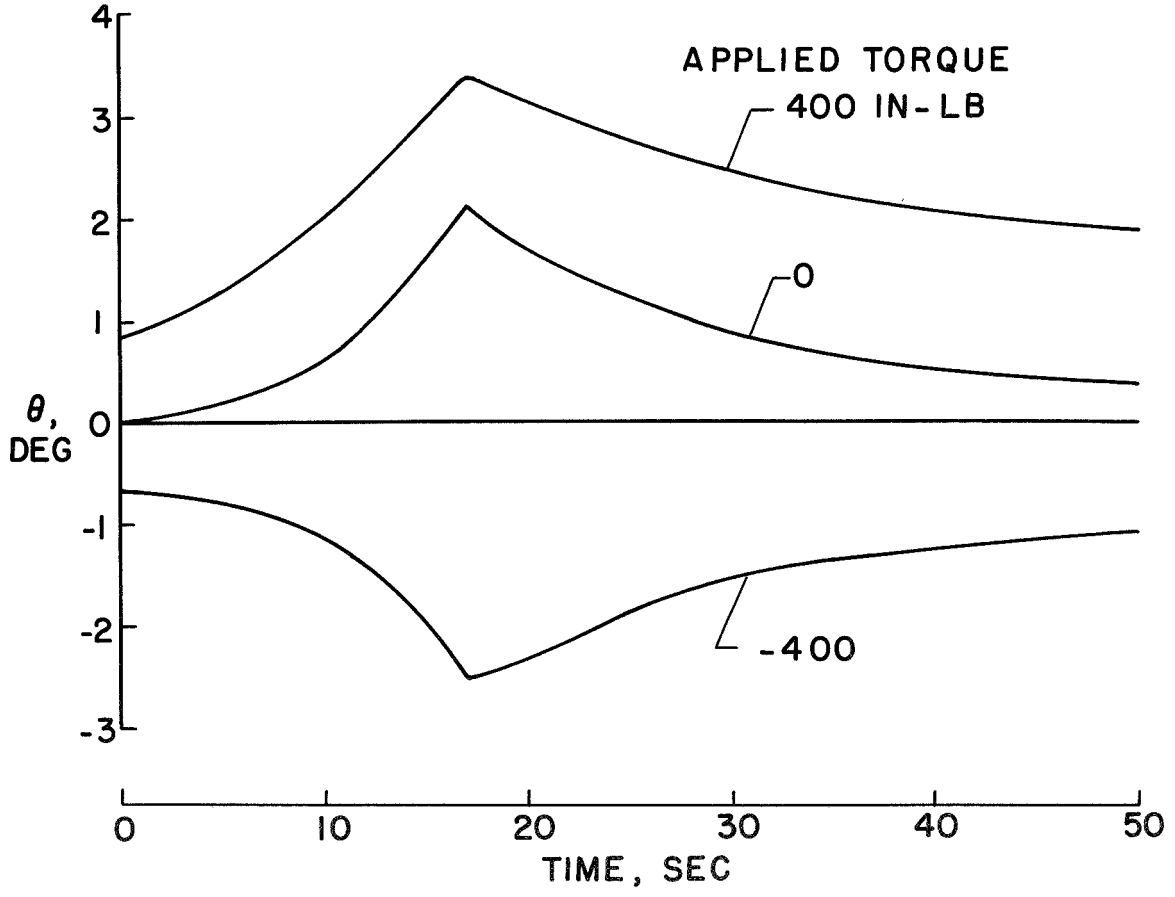

Figure 6.- Measured tip-rotation histories for applied torques of 0 and ±400 in-lb.

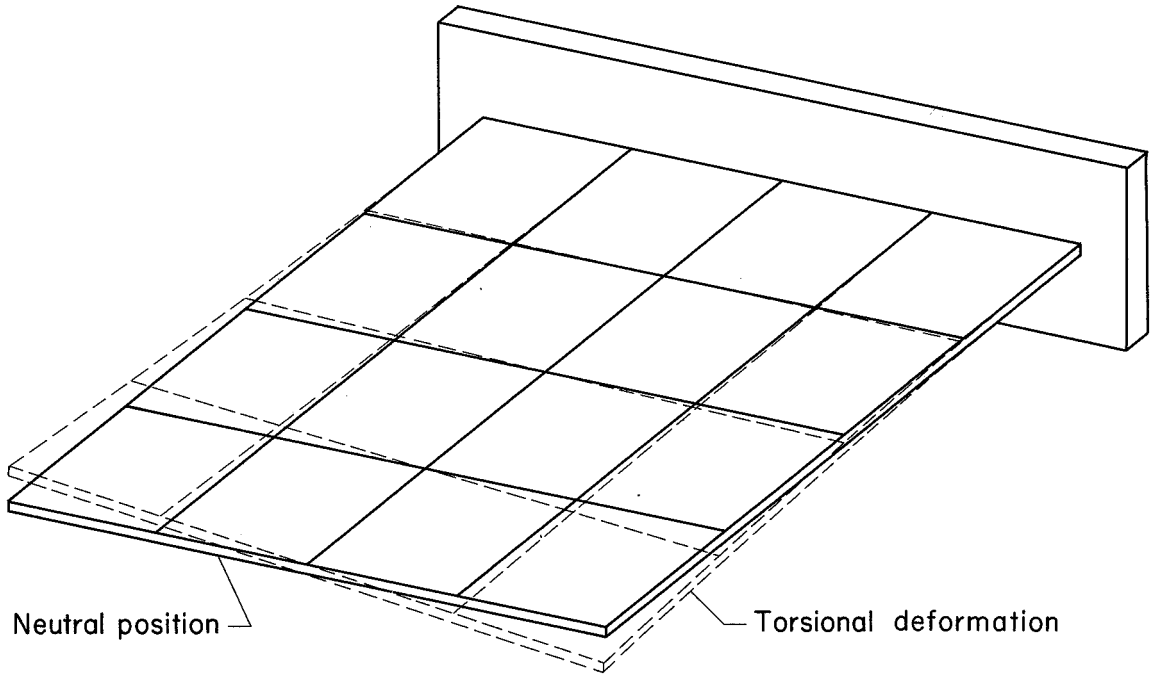

Figure 7.- Torsional deformation of plate subjected to rapid edge heating.

cooled, the deformations decreased and the plate returned to its original position. The same type and direction of deformation was obtained regardless of whether heat was applied symmetrically, on either edge, or simultaneously to the upper surface of the plate along one edge and to the lower surface along the other edge, and conversely because of an initial curvature of the plate resembling the torsional deformation shown in figure 7. Note that the plate underwent an appreciable deformation without the application of an external load. This is a thermal buckling phenomenon (see ref. 2) which may be a significant factor in the control of missiles having solid fins. The increased deformations, which occurred when a constant torque was applied in the same direction as the initial twist, indicate an approximate superposition of the deformation induced by the thermal stresses on the initial static deflection. When a torque was applied in the opposite direction, the plate twisted in the direction of the applied torque, but the maximum twist was slightly less.

B. Natural Frequencies

It is difficult to detect the frequency changes of a plate under transient heating conditions because of the time required to establish resonance. For this reason the investigation was limited to the first bending and first torsion modes, inasmuch as each of these modes could be excited by striking the plate in the proper manner. The first bending mode is easily produced by striking the plate at the midchord line near the tip. To excite the first torsion mode, the plate was held

with one hand at the tip midchord and then struck at a free corner. The plate was then released. Since the midchord line is a node of the first torsion mode, by holding the plate at this point for an instant after it has been struck, most bending vibrations are damped out and (as dynamic strain-gage records indicated) practically pure torsion remains. Frequency measurements were made by recording the output from a two active-arm bridge made up from two Baldwin SR-4 Type BNF-7D (+50 to +250) wire strain gages placed back to back on opposite sides of the plate in the position shown in figure 3. Various gage positions were tried and the one shown was found to give the best output for the modes tested.

Figure 8 shows how the frequencies of the first two modes varied during the test. Here, frequency of vibration in cycles per second has been plotted against time in seconds for the first bending and first torsion modes. The first bending frequency decreased from 19 cycles per second to 15 cycles per second at the point of maximum temperature gradient. This is a 21-percent reduction in frequency. The first torsion frequency begins at 48 cycles per second and drops to a minimum of 30 cycles per second - a reduction in natural frequency of about 35 percent. As the plate cools, both frequencies return to their original values. The small irregularity which occurs at the peak of the heating cycle has been observed in all the first torsion mode tests,

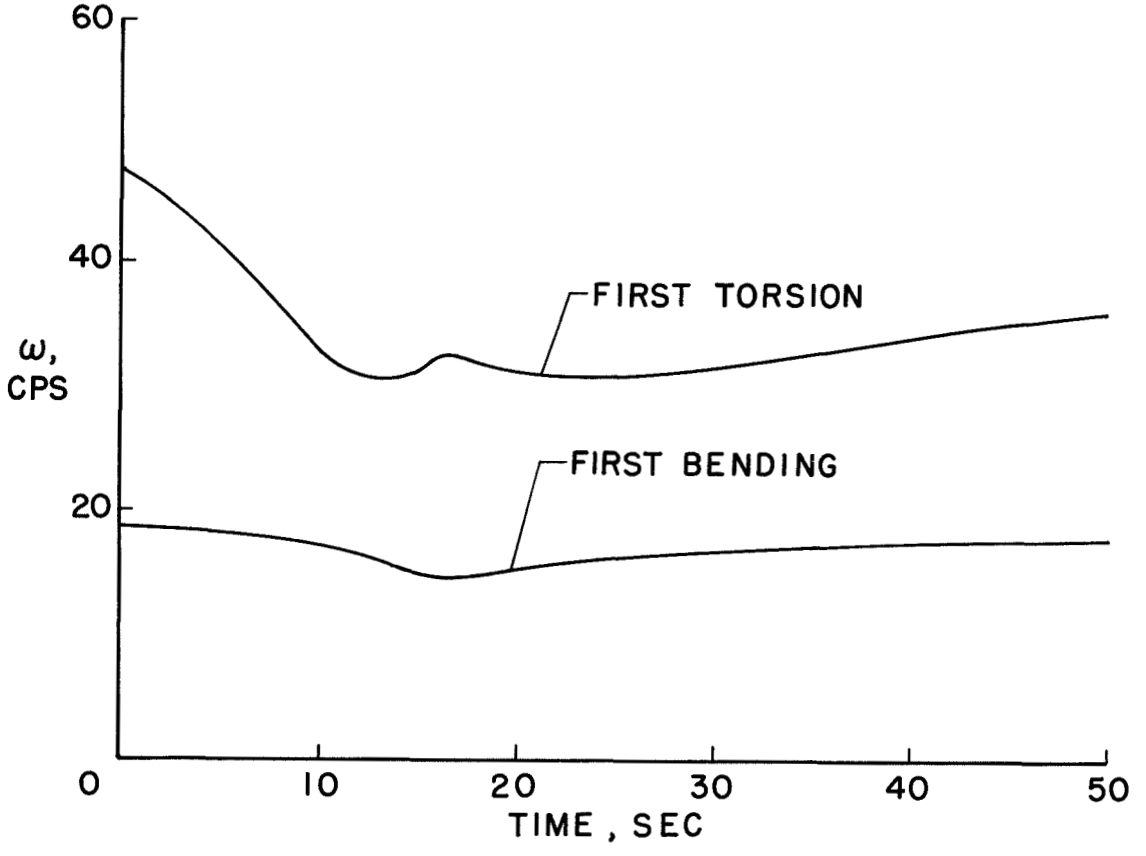

Figure 8.- Measured frequency histories for the first bending and first torsion modes.

but as yet its cause has not been determined.

In addition to the effects of thermal stresses, the behavior of the plate may also be affected by changes in the material properties. At 300° F the modulus of elasticity decreases about 7 percent (ref. 3) and the coefficient of thermal expansion increases about 6 percent (ref. 4). No information has been found for values of Poisson's ratio or the shear modulus at elevated temperatures. Only a very small portion of the plate reaches or exceeds 300° F during a test, therefore, the changes in material properties would have only a small effect on the deformations and natural frequencies and the changes measured in these tests may be attributed to the induced thermal stresses.

DECLASSIFIED

IV. COMPARISON OF THEORETICAL CALCULATIONS WITH EXPERIMENTAL RESULTS

As a first approach to predicting the changes measured in these tests, small-deflection theory has been used. The analytical approach, which is a combination of the energy methods used to solve buckling and vibrational problems, is outlined in the Appendix.

A. Deformations

A comparison of the predicted and actual effect of the temperature gradient on the torsional stiffness for the case of no vibration is shown in figure 9. Here the tip rotation in degrees has been plotted against the edge-to-center temperature difference ΔT in degrees Fahrenheit for an applied torque of 400 inch-pounds. Curves are shown for the period of heating (or increasing ΔT) and cooling (or decreasing ΔT). The small-deflection theory gives a reasonable approximation of the reduction in stiffness about halfway to the buckling temperature predicted by the theory. Above this point, however, the small-deflection theory indicates that the plate deflections would increase more rapidly than actually occurs.

B. Natural Frequency

Figure 10 compares the results of the calculations with test results when there are no external loads and the plate is vibrating in the first torsion mode. In this figure the frequency in cycles per second has been plotted against temperature difference between the edge

DECLASSIFIED

DECLASSIFIED

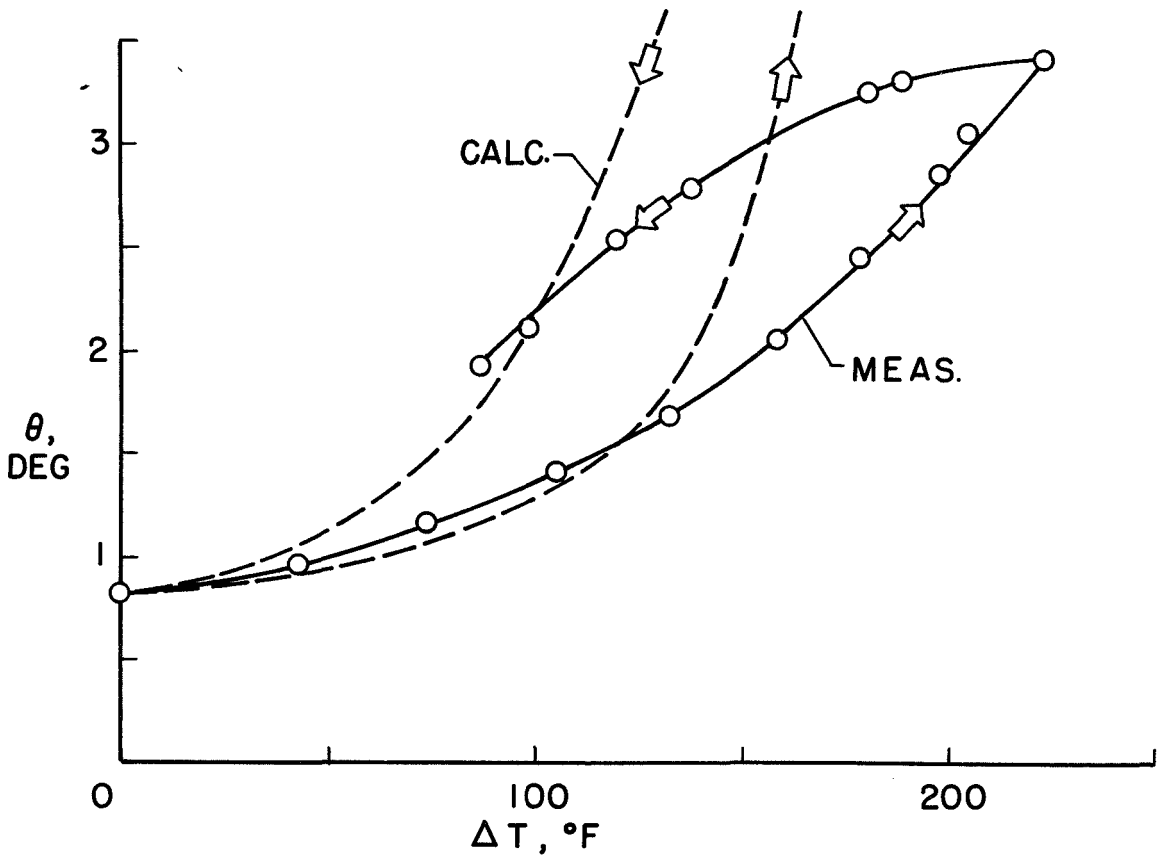

Figure 9.- Comparison of measured and calculated tip rotations for an applied torque of 400 in-lb.

DECLASSIFIED

DECLASSIFIED

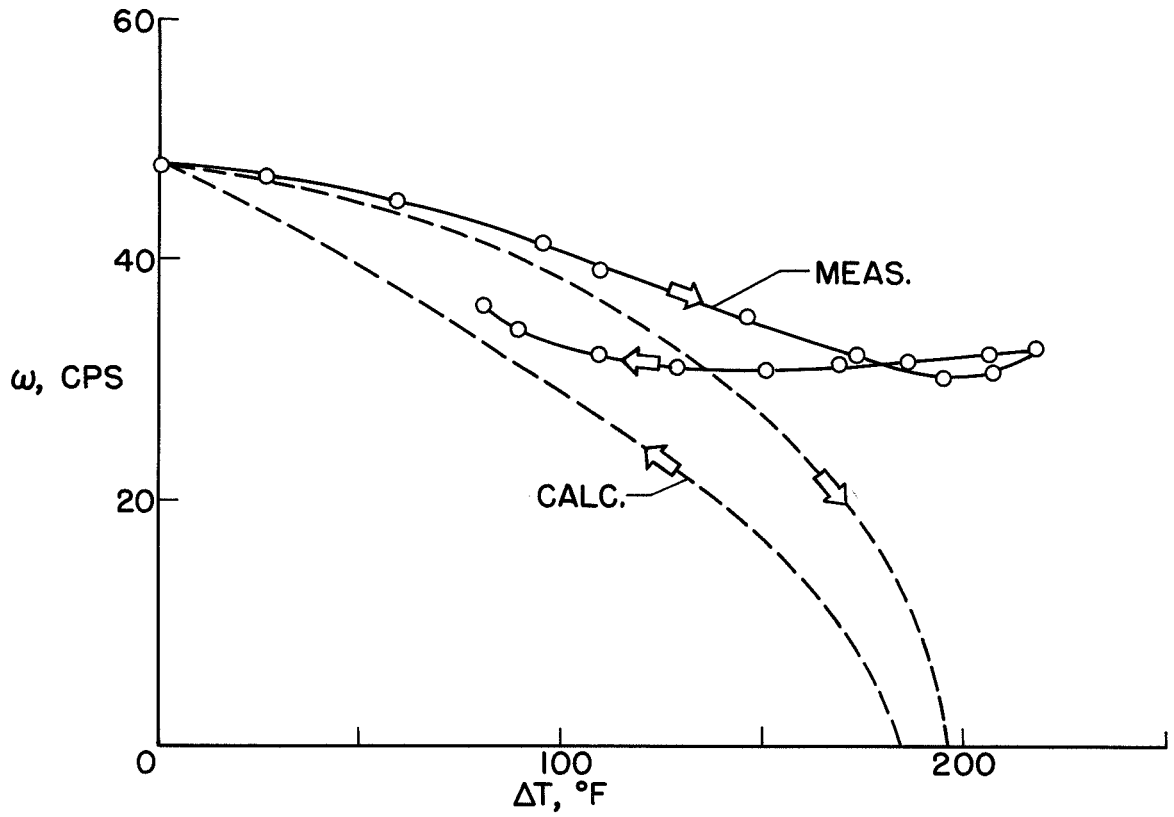

Figure 10.- Comparison of measured and calculated frequency changes for the first torsion mode.

DECLASSIFIED

and the midchord line for the periods of increasing and decreasing ΔT. The small-deflection theory again approximates the frequency change about halfway to the critical buckling temperature. Above this value, the theory again overestimates the change. This disagreement is expected since the measured deflection of a corner is approximately equal to the plate thickness. For deflections of this magnitude, the small-deflection theory is no longer valid.

Figure 11 shows a similar comparison of measured and calculated frequency as a function of time. The ratio of actual frequency to the initial uniform-temperature frequency is plotted against time in seconds. The calculated curve indicates that the theoretical critical-buckling temperature differential is reached in about 15 seconds. The small-deflection theory predicts that the plate would have lost all its stiffness at this point, but this is not the actual case. Since stiffness is proportional to the square of the frequency, the frequency decrease obtained indicates that only about half of the stiffness was lost as a result of the induced thermal stresses. As the plate cools and the temperature difference becomes less than half that required for buckling, the theory is again in fair agreement with the test results.

DECLASSIFIED

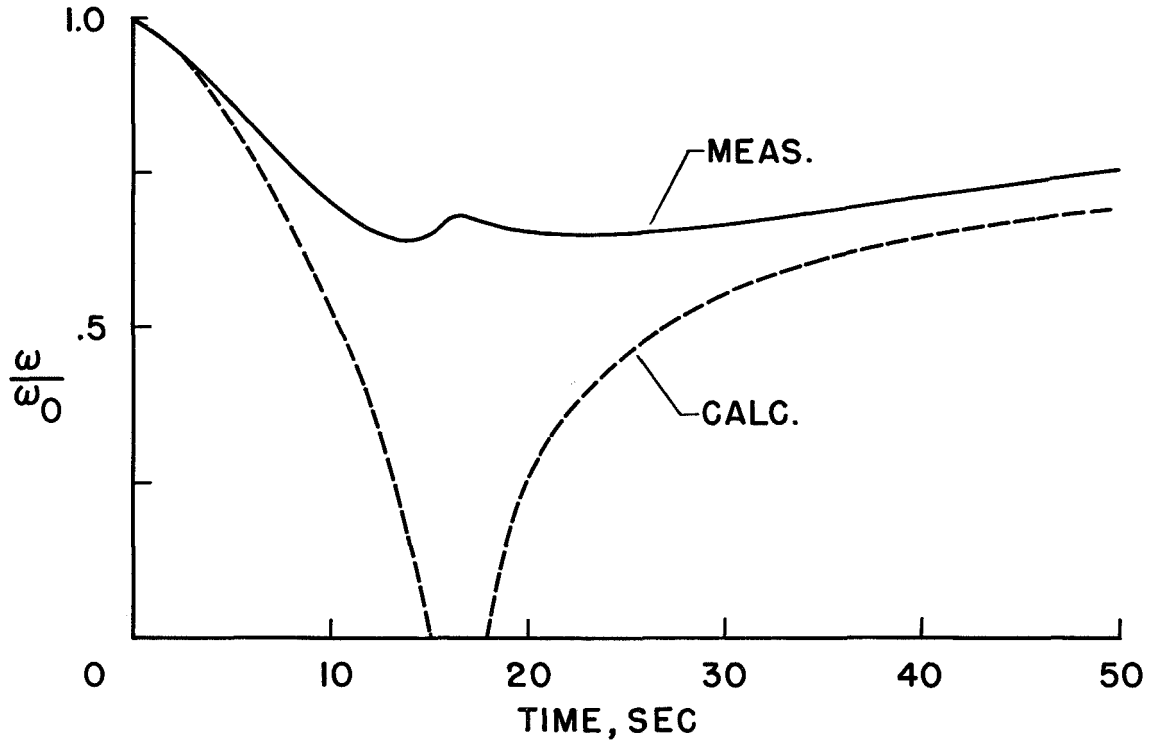

Figure 11.- Comparison of measured and calculated frequency histories for the first torsion mode.

DECLASSIFIED

V. CONCLUDING REMARKS

Tests of a cantilever plate have shown that the midplane stresses imposed by a nonuniform temperature distribution can effectively reduce the stiffness of the plate. This reduction in stiffness is reflected in the increased deformation under the action of a constant applied torque and also in the reduction of the natural frequency of vibration of the first two modes of the plate. By using small-deflection theory and by employing energy methods, the effect of nonuniform heating on the plate stiffness was calculated. The theory predicts the general effects of the thermal stresses, but is inadequate when the deformations become large. An extension of the analysis to account properly for large deflections would be expected to give more satisfactory results near the critical temperature.

VI. ACKNOWLEDGEMENTS

The author wishes to express his gratitude to the National Advisory Committee for Aeronautics for the use of their equipment and personnel in carrying out the testing program.

He also wishes to thank Mr. R. R. Heldenfels of the NACA for his assistance and guidance throughout the program and especially in the theoretical analysis, Mr. K. E. Fuller of the NACA for his help in conducting the tests, and Professor H. J. Huffington and other members of the Applied Mechanics Staff of Virginia Polytechnic Institute for their assistance in the preparation of this thesis.

VII. REFERENCES

1. Kaye, Joseph: The Transient Temperature Distribution in a Wing Flying at Supersonic Speeds. Jour. Aero. Sci., Vol. 17, No. 12, Dec. 1950, pp. 737-607, 616.

2. Gossard, M. L., Seide, P., and Roberts, W. M.: Thermal Buckling of Plates. NACA TN 2771, 1952.

3. Blanchard, A. F., Tedesco, L. F., and Dorn, J. E.: Compressive Properties of Aluminum Alloy Sheet at Elevated Temperatures. Proc. Am. Soc. for Testing Mat., Vol. 46, 1946, pp. 951-967.

4. Alcoa Aluminum and Its Alloys. Aluminum Company of America, 1947.

5. Timoshenko, S., and Goodier, J. N.: Theory of Elasticity. Second Ed., McGraw-Hill Book Co., 1951, pp. 155, 169.

6. Heldenfels, Richard R., and Roberts, William M.: Experimental and Theoretical Determination of Thermal Stresses in a Flat Plate. NACA TN 2769, 1952.

7. Love, A. E. H.: A Treatise on the Mathematical Theory of Elasticity, Fourth Ed., Dover Publications, 1944, p. 95.

8. Timoshenko, S.: Theory of Elastic Stability. McGraw-Hill Book Co., Inc., 1936, pp. 305-323.

9. Timoshenko, S.: Vibration Problems in Engineering. Second Ed., D. Van Nostrand Co., Inc., 1937, p. 423.

10. Grant, F. S.: A Short Method for Evaluating Determinants and Solving Systems of Linear Equations with Real or Complex Coefficients. Am. Inst. Elec. Eng. Trans., Vol. 60, 1941, pp. 1235-1240.

VIII. VITA

The author was born on May 30, 1931 in Michigan City, Indiana, and received his primary and secondary education in the Indiana public schools. He attended Purdue University in Lafayette, Indiana, and received a Bachelor of Science degree in Civil Engineering on June 1, 1952. Since June 19, 1952 he has been employed by the National Advisory Committee for Aeronautics at Langley Field, Virginia.

Louis P. Vosteen

IX. APPENDIX

SMALL-DEFLECTION ANALYSIS OF CANTILEVER PLATE SUBJECTED TO NONUNIFORM TEMPERATURE DISTRIBUTION

By using small-deflection theory and by making several simplifying assumptions, an analysis of the effect of rapid heating on the deformations, natural frequencies of vibration, and torsional stiffness of a cantilever plate was made. The method used is outlined in this appendix. Figure 12 shows the plate geometry.

Symbols

a	plate length, in.
A_{mn}, A_{ij}	arbitrary coefficients of deflection function
b	plate half-width, in.
C_{mn}	coefficients of matrix equation
C	torsional stiffness, lb-in.^{2}
C_e	effective torsional stiffness, lb-in.^{2}
D	plate flexural stiffness, $\frac{Et^3}{12(1 - \mu^2)}$
E	Young's modulus, psi
F	concentrated load, lb
g	gravitational constant, in/sec^2
G	modulus of elasticity in shear, psi
K	arbitrary coefficient of stress function

p	distributed load, psi
t	plate thickness, in.
T	temperature, $^{\circ}F$
T_0	temperature of midchord, $^{\circ}F$
ΔT	difference in temperature between edge and midchord, $^{\circ}F$
ΔT_{cr}	critical temperature difference, $^{\circ}F$
U_B	potential energy of bending, in-lb
U_H	strain energy due to thermal expansion, in-lb
U_L	potential energy due to external load, in-lb
U_M	energy due to midplane stresses, in-lb
U_S	strain energy of midplane stresses, in-lb
$\omega^2 U_V$	kinetic energy of vibration, in-lb
w	deflection, in.
x	longitudinal coordinate measured from root, in.
y	transverse coordinate measured from midchord line, in.
α	coefficient of thermal expansion, $\frac{\text{in.}}{\text{in.} - {}^{\circ}F}$
ϵ_x	longitudinal strain, in./in.
ϵ_y	transverse strain, in./in.
γ_{xy}	shearing strain, in./in.
ζ	arbitrary exponent in temperature distribution
θ	tip rotation, deg
θ_0	tip rotation when $\Delta T = 0$, deg

μ	Poisson's ratio
γ	specific weight, lb/cu in.
σ_x	longitudinal direct stress, psi
σ_y	transverse direct stress, psi
τ_{xy}	shear stress, psi
ϕ	stress function
ω	frequency, cps
ω_0	frequency when $\Delta T = 0$, cps

A. Temperature Distribution

The temperature is assumed to be constant through the thickness of the plate and along the span; the distribution across the chord is represented by the simple power law

$$T = T_0 + \Delta T(y/b)^{\zeta} \tag{1}$$

which involves the edge to midchord temperature difference ΔT and the power ζ required to describe the measured chordwise temperature distribution. The power ζ, which varies during a test, determines how sharply the temperature rises near the edges of the plate. In order to find how ζ varied, a curve of the form given in equation (1) was fitted to the chordwise temperature distribution measured at various times during a test. At the start of heating ζ is very large, but it decreases to about 6 at the peak edge temperature, continues to drop as

DECLASSIFIED

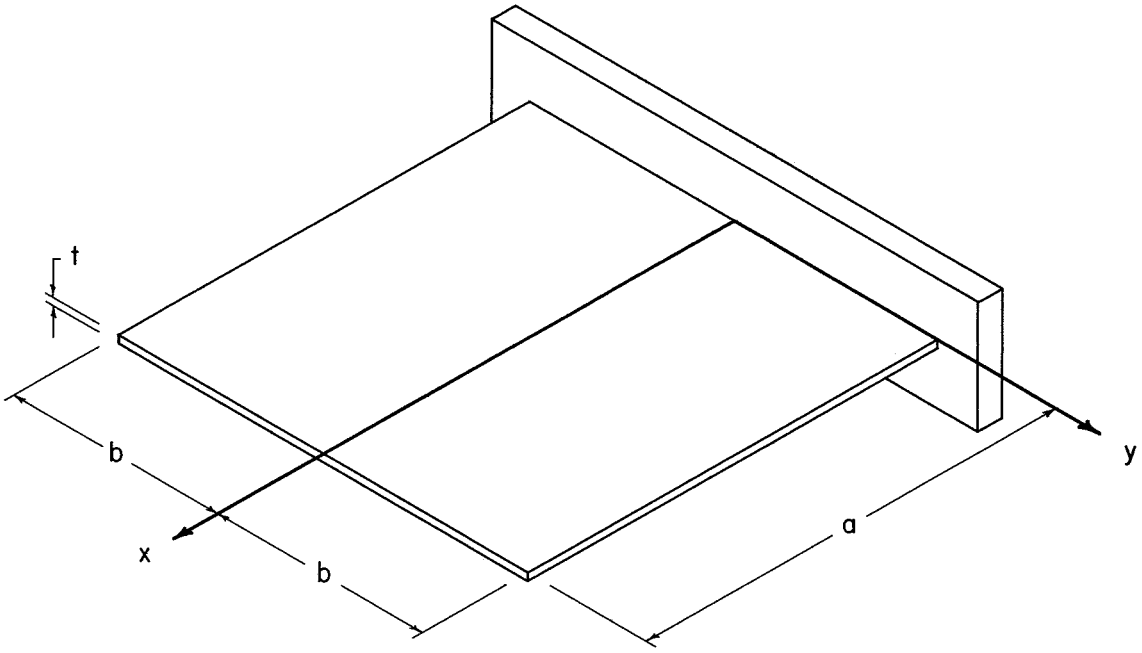

Figure 12.- Dimensions and coordinate system of cantilever plate.

DECLASSIFIED

the plate cools, and reaches a value of 2 at the end of the test (about 35 seconds after the peak temperature). The temperature distribution given by equation (1) fits the measured distribution rather well during heating as can be seen from figure 13, but becomes increasingly poor as the plate cools.

B. Thermal Stresses

The plate is assumed to be in a state of plane stress and all stresses are assumed to be in the elastic range of the material. The assumption also has been made that the material properties of the plate do not change with temperature. Thermal stresses are given by the relationships

$$\left.\begin{aligned} \sigma_x &= \frac{\partial^2 \phi}{\partial y^2} \\ \sigma_y &= \frac{\partial^2 \phi}{\partial x^2} \\ \tau_{xy} &= -\frac{\partial^2 \phi}{\partial x \partial y} \end{aligned}\right\} \qquad (2)$$

where ϕ is the Airy stress function (see ref. 5) assumed to be given by

$$\phi = KE\alpha\Delta T(x^2 - a^2)^2(y^2 - b^2)^2 \qquad (3)$$

This function satisfies the boundary condition that the stresses

DECLASSIFIED

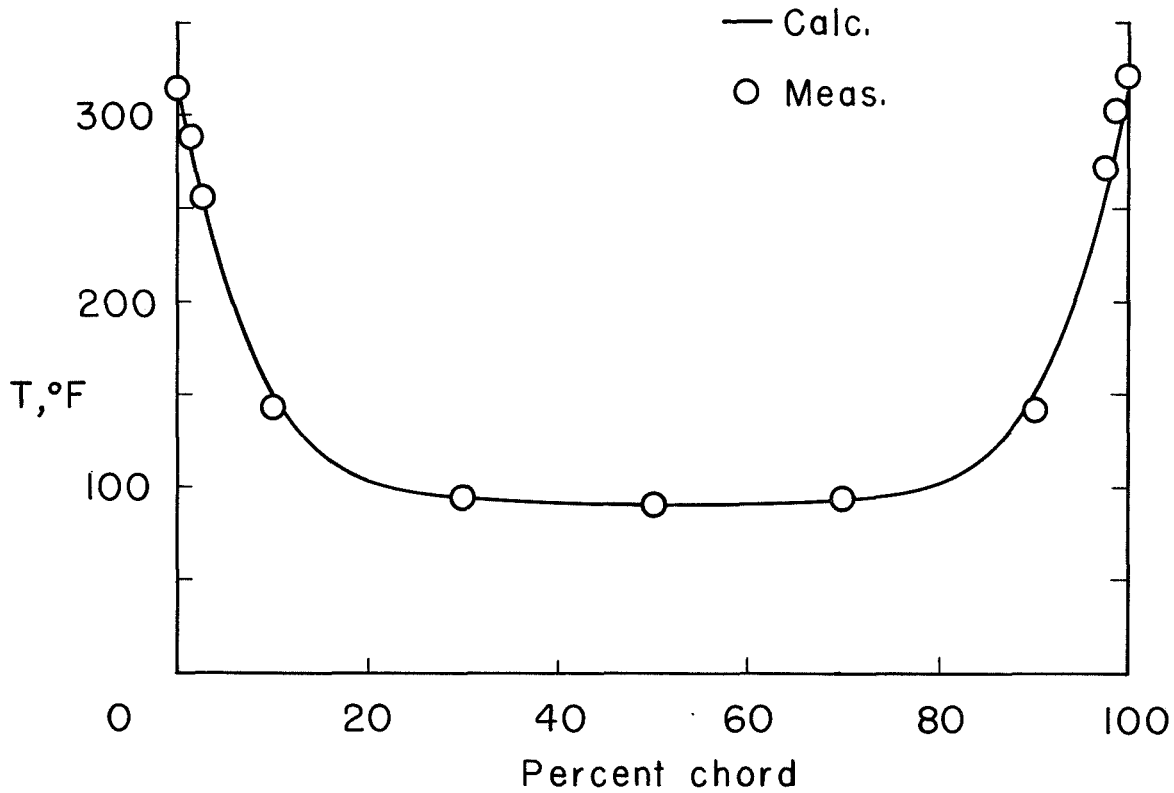

Figure 13.- Comparison of measured and calculated chordwise temperature distributions at the time of maximum edge temperature.

DECLASSIFIED

(equations 2) vanish on the free boundaries ($x = a$ and $y = \pm b$). The distribution of stress as given by equations (2) and (3) has been plotted in figure 14 in dimensionless form for a square plate ($a/b = 2$).

To evaluate the arbitrary constant in the stress function (equation (3)) the method of minimum complementary energy is used. The expression can be written simply as

$$\frac{\partial}{\partial K}(U_S + U_H) = 0 \tag{4}$$

where

$$U_S = \frac{1}{2E}\int_0^a\int_{-b}^b \left[\sigma_x^2 + \sigma_y^2 - 2\mu\sigma_x\sigma_y + 2(1 + \mu)\tau_{xy}^2\right] dx\, dy \tag{5}$$

$$U_H = \int_0^a\int_{-b}^b \alpha T(\sigma_x + \sigma_y)\, dx\, dy \tag{6}$$

The first integral is the usual strain-energy expression and the second represents the strain energy due to thermal expansion of the plate. Equations (5) and (6) have been used by previous investigators (see, for example, ref. 6) and will be shown to be valid since the derivative of the strain energy with respect to each of the stress components gives the corresponding strain component (ref. 7).

DECLASSIFIED

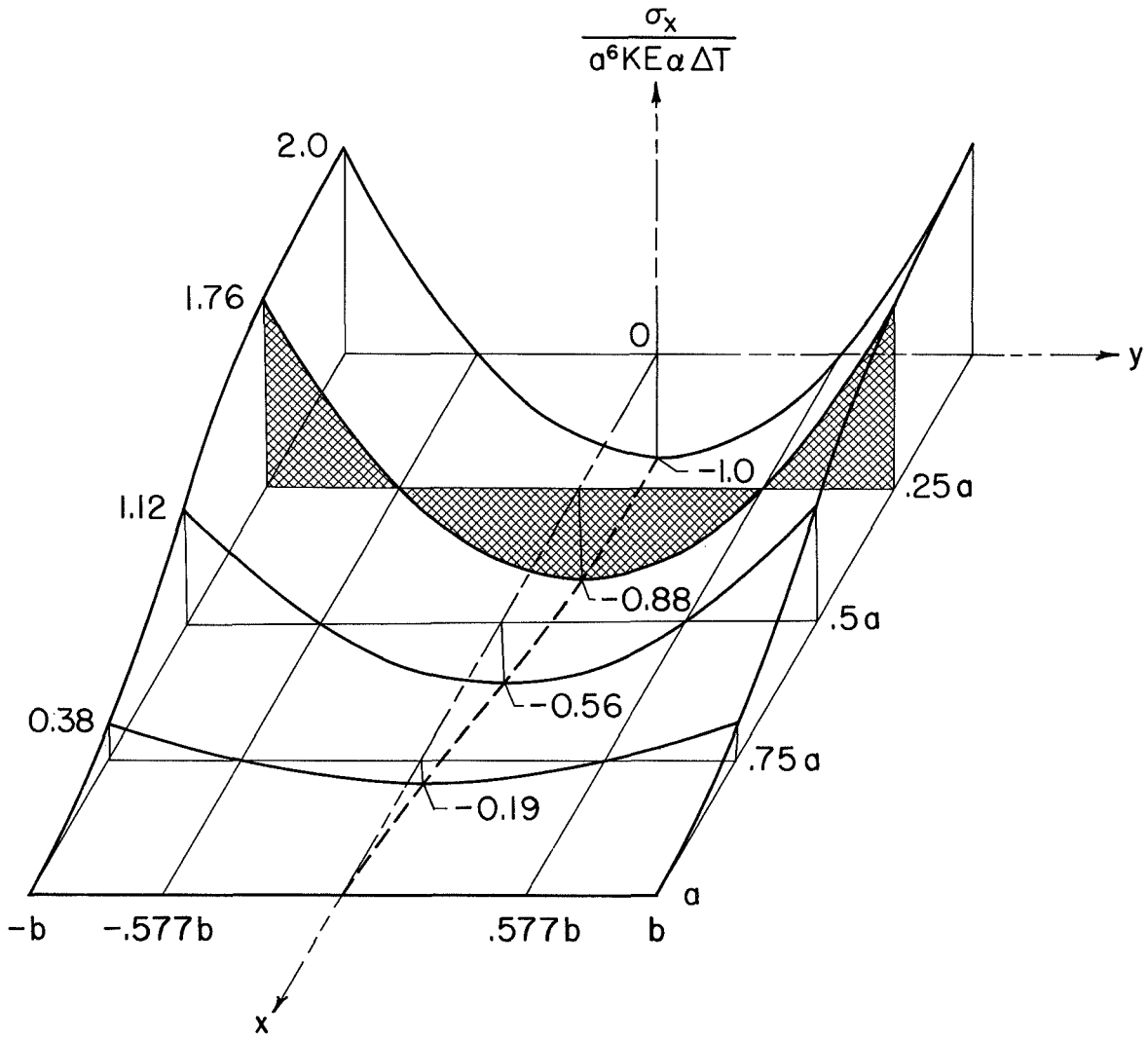

(a) Longitudinal direct stress.

Figure 14.- Assumed thermal stress distributions in a cantilever plate rapidly heated along the longitudinal edges.

DECLASSIFIED

DECLASSIFIED

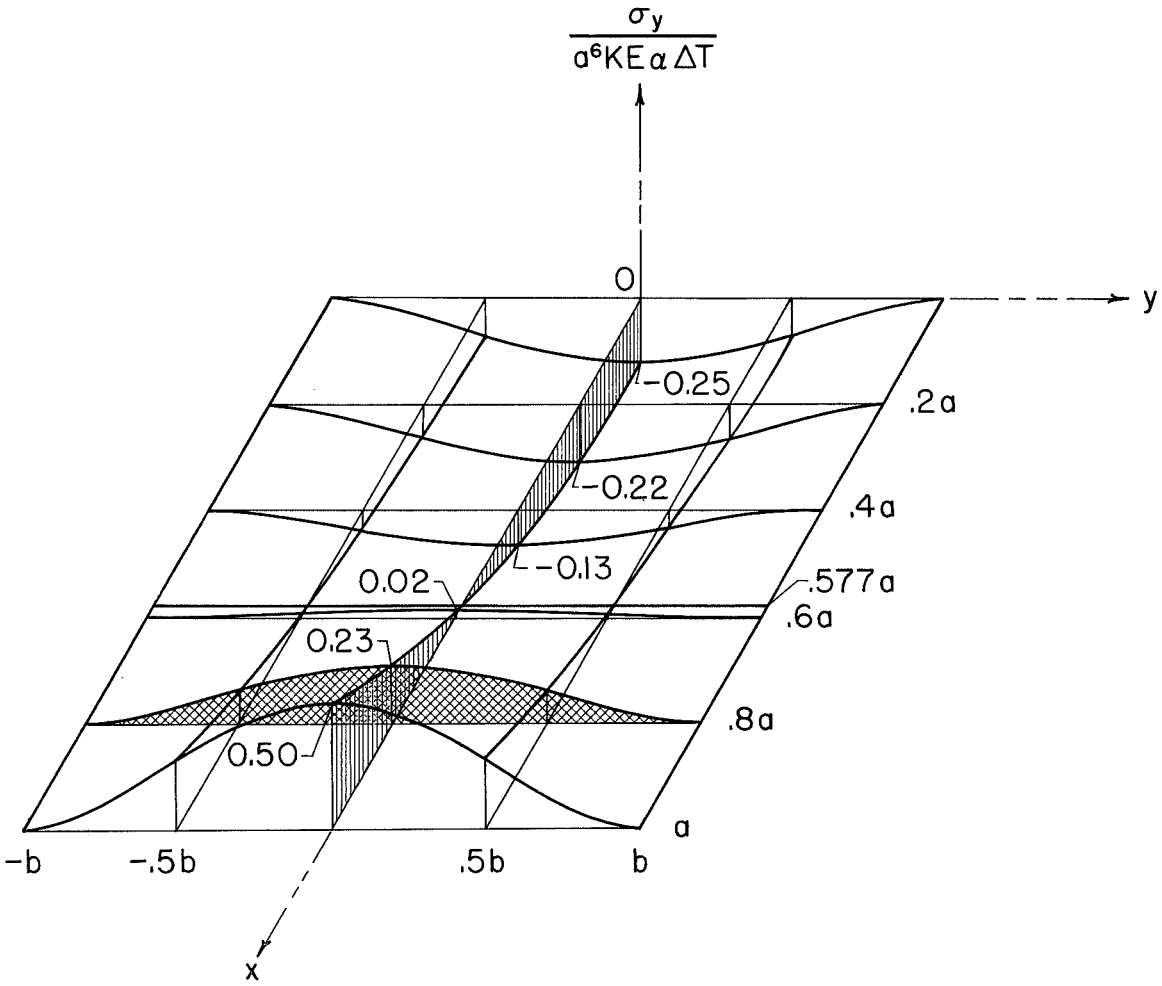

(b) Transverse direct stress.

Figure 14.- Continued.

DECLASSIFIED

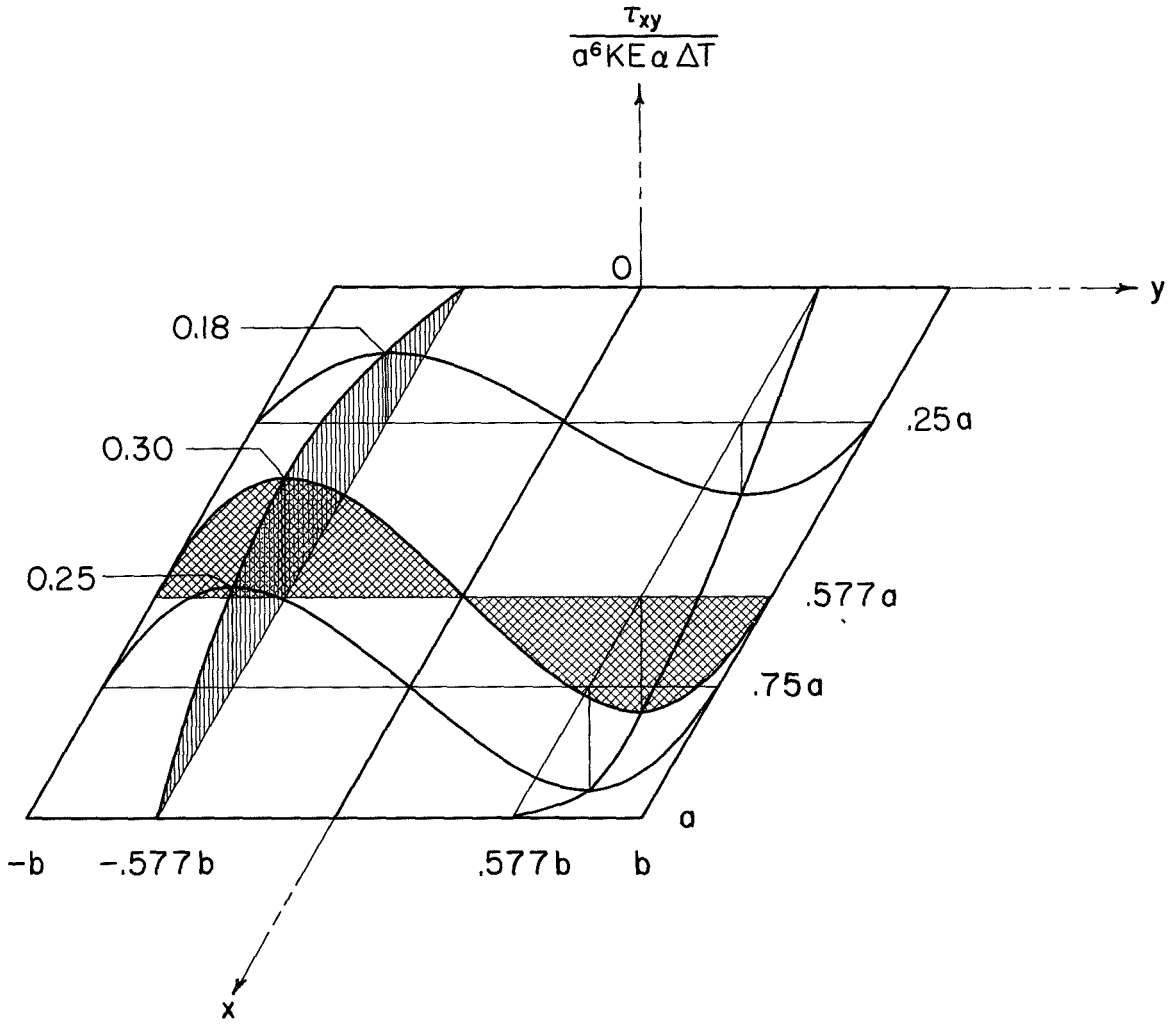

(c) Shear stress.

Figure 14.- Concluded.

DECLASSIFIED

The stress-strain relations are

$$\epsilon_x = \frac{1}{E}(\sigma_x - \mu\sigma_y) + \alpha T \qquad (a)$$

$$\epsilon_y = \frac{1}{E}(\sigma_y - \mu\sigma_x) + \alpha T \qquad (b)$$

$$\gamma_{xy} = \frac{1}{G}\tau_{xy} = \frac{2(1 + \mu)}{E}\tau_{xy} \qquad (c)$$

and the strain energy per unit volume as given by equations (5) and (6) is.

$$\frac{1}{2E}\left[\sigma_x^2 + \sigma_y^2 - 2\mu\sigma_x\sigma_y + 2(1 + \mu)\tau_{xy}^2 + 2E\alpha T(\sigma_x + \sigma_y)\right] \qquad (d)$$

The derivative of the strain energy with respect to σ_x is

$$\frac{1}{2E}(2\sigma_x - 2\mu\sigma_y + 2E\alpha T) \qquad (e)$$

Equation (e) may then be reduced to

$$\frac{1}{E}(\sigma_x - \mu\sigma_y) + \alpha T \qquad (f)$$

which is the longitudinal strain as given by equation (a).

In a similar manner it may be shown that the derivatives of the strain energy with respect to the other stress components give their corresponding strain components. It may be concluded, therefore,

DECLASSIFIED

DECLASSIFIED

that the strain-energy expressions given in equations (5) and (6) are valid.

By using equation (1) for temperature and equations (2) and (3) for the stresses, equation (5) may be rewritten as

$$U_S = 8k(K\alpha\Delta T)^2 f(x,y) \tag{7}$$

where

$$\left.\begin{aligned} f(x,y) = \int_0^a \int_{-b}^b \Big[& (x^2 - a^2)^4(3y^2 - b^2)^2 + (3x^2 - a^2)^2(y^2 - b^2)^4 - \\ & 2\mu(3x^2 - a^2)(x^2 - a^2)^2(3y^2 - b^2)(y^2 - b^2)^2 + \\ & 32(1 + \mu)x^2y^2(x^2 - a^2)^2(y^2 - b^2)^2 \Big] dx\, dy \end{aligned}\right\} \tag{8}$$

and equation (6) becomes

$$U_H = 4KE(\alpha\Delta T)^2 g(x,y) \tag{9}$$

where

$$\begin{aligned} g(x,y) = \int_0^a \int_{-b}^b \left[\frac{T_0}{\Delta T} + \left(\frac{y}{b}\right)^5\right] \Big[& (x^2 - a^2)^2(3y^2 - b^2) + \\ & (3x^2 - a^2)(y^2 - b^2)^2 \Big] dx\, dy \end{aligned} \tag{10}$$

Equation (4) can now be written

DECLASSIFIED

DECLASSIFIED

$$\frac{\partial}{\partial K}\left[\delta\alpha(K\alpha\Delta T)^2 f(x,y) + 4K\delta(\alpha\Delta T)^2 g(x,y)\right] = 0 \tag{11}$$

which reduces to

$$4Kf(x,y) + g(x,y) = 0 \tag{12}$$

By evaluating the expressions for $f(x,y)$ and $g(x,y)$ from equations (8) and (10) and substituting these quantities into equation (12), the value of K is then determined. This value is

$$K = -\frac{735}{2a^6\left[7\left(\frac{a}{b}\right)^4 + 4\left(\frac{a}{b}\right)^2 + 7\right]}\,\frac{\zeta}{(\zeta + 3)(\zeta + 1)} \tag{13}$$

When $a/b = 2$, equation (13) reduces to

$$K = -\frac{2.72}{a^6}\,\frac{\zeta}{(\zeta + 3)(\zeta + 1)} \tag{14}$$

Since the value of K is negative, a positive value of the stress parameters shown in figure 14 actually indicates a negative or (for σ_x and σ_y) compressive stress.

DECLASSIFIED

DECLASSIFIED

C. Effect of Temperature Gradient on Deflections and Natural Frequencies

To find the effect of temperature gradient on the deflections and natural frequencies, another minimum-energy method is used. Deflections are represented by the power series

$$w = \sum_{m=1}^{\infty} \sum_{n=1}^{\infty} A_{mn} x^{m+1} y^{n-1} \tag{15}$$

which satisfies the boundary conditions that the slope and deflection are zero at the root, $x = 0$. The undetermined coefficients of the deflection function may be evaluated by minimizing the change in energy during deflection with respect to each of these coefficients. The variation in the change in energy is expressed as

$$\frac{\partial}{\partial A_{ij}}\left(U_B + U_M - \omega^2 U_V + U_L\right) = 0 \tag{16}$$

where

$$U_B = \frac{D}{2}\int_0^a \int_{-b}^{b} \left[\left(\frac{\partial^2 w}{\partial x^2}\right)^2 + \left(\frac{\partial^2 w}{\partial y^2}\right)^2 + 2\mu\left(\frac{\partial^2 w}{\partial x^2}\,\frac{\partial^2 w}{\partial y^2}\right) + 2(1-\mu)\left(\frac{\partial^2 w}{\partial x \partial y}\right)^2\right] dx\, dy \tag{17}$$

$$U_M = \frac{t}{2}\int_0^a \int_{-b}^{b} \left[\sigma_x\left(\frac{\partial w}{\partial x}\right)^2 + \sigma_y\left(\frac{\partial w}{\partial y}\right)^2 + 2\tau_{xy}\,\frac{\partial w}{\partial x}\,\frac{\partial w}{\partial y}\right] dx\, dy \tag{18}$$

DECLASSIFIED

DECLASSIFIED

$$U_V = \frac{2n^2\gamma t}{g} \int_0^a \int_{-b}^b w^2 \, dx \, dy \tag{19}$$

$$U_L = \int_0^a \int_{-b}^b pw \, dx \, dy \tag{20}$$

The first integral is the energy due to bending, the second is the energy imposed by midplane thermal stresses (obtained from equations (2) and (3)), the third is the kinetic energy of vibration, and the fourth is the energy resulting from any external loads applied perpendicular to the plane of the plate. (See refs. 8 and 9.) By using equations (2) and (3) for stresses and equation (14) for deflections, equations (16), (17), and (18) may be written

$$\left.\begin{aligned} U_B = \frac{D}{2}\int_0^a \int_{-b}^b \sum_{m=1}^{\infty}\sum_{n=1}^{\infty} \Bigg\{ & \Big[A_{mn} m(m+1)x^{m-1}y^{n-1}\Big]^2 + \\ & \Big[A_{mn}(n-1)(n-2)x^{m+1}y^{n-3}\Big]^2 + \\ & 2\mu\Big[A_{mn} m(m+1)x^{m-1}y^{n-1}\Big]\Big[A_{mn}(n-1)(n-2)x^{m+1}y^{n-3}\Big] + \\ & 2(1-\mu)\Big[A_{mn}(m+1)(n-1)x^{m}y^{n-2}\Big]^2 \Bigg\} dx \, dy \end{aligned}\right\} \tag{21}$$

DECLASSIFIED

DECLASSIFIED

$$U_M = \frac{t}{2}\int_0^a\int_{-b}^b\sum_{m=1}^{\infty}\sum_{n=1}^{\infty}\Big\{4KE\alpha\Delta T(x^2 - a^2)^2(3y^2 - b^2)\Big[A_{mn}(m + 1)x^m y^{n-1}\Big]^2 + 4KE\alpha\Delta T(3x^2 - a^2)(y^2 - b^2)^2\Big[A_{mn}(n - 1)x^{m+1}y^{n-2}\Big]^2 + 32KE\alpha\Delta Txy(x^2 - a^2)(y^2 - b^2)\Big[A_{mn}(m + 1)x^m y^{n-1}\Big]\Big[A_{mn}(n - 1)x^{m+1}y^{n-2}\Big]\Big\}dx\,dy \tag{22}$$

$$U_V = \frac{2\pi^2\gamma t}{g}\int_0^a\int_{-b}^b\Big[A_{mn}x^{m+1}y^{n-1}\Big]^2\,dx\,dy \tag{23}$$

If the external loading consists of a couple formed by applying concentrated loads F at the free corners ($x = a$, $y = \pm b$), equation (19) becomes

$$U_L = F(w_{a,b} - w_{a,-b})$$

or

$$U_L = F\sum_{m=1}^{\infty}\sum_{n=1}^{\infty}A_{mn}a^{m+1}\Big[b^{n-1} - (-b)^{n-1}\Big] \tag{24}$$

When equations (21-24) incl. are minimized with respect to the arbitrary coefficient A_{ij}, and the indicated integrations are performed, the following general equation is obtained.

DECLASSIFIED

DECLASSIFIED

$$
\begin{aligned}
&\sum_{m=1}^{\infty}\sum_{n=1}^{\infty} A_{mn}\Bigg\{\frac{mi(m+1)(i+1)a^{m+i-1}}{(m+i-1)(n+j-1)}\left[b^{n+j-1}-(-b)^{n+j-1}\right]+ \\
&\frac{(n-1)(n-2)(j-1)(j-2)}{(m+i+3)(n+j-5)}\,a^{m+i+3}\left[b^{n+j-5}-(-b)^{n+j-5}\right]+ \\
&\mu\left(\frac{m(m+1)(j-1)(j-2)+i(i+1)(n-1)(n-2)}{(m+i+1)(n+j-3)}\,a^{m+i+1}\left[b^{n+j-3}-\right.\right. \\
&\left.\left.(-b)^{n+j-3}\right]\right)+2(1-\mu)\frac{(m+1)(i+1)(j-1)(n-1)}{(m+i+1)(n+j-3)}\,a^{m+i+1}\left[b^{n+j-3}-\right. \\
&\left.(-b)^{n+j-3}\right]+6h\,\frac{\alpha E m\Delta T}{D}\,a^{m+i+5}\left[b^{n+j+1}-(-b)^{n+j+1}\right]\times \\
&\Bigg[\frac{(m+1)(i+1)(n+j-2)}{(m+i+5)(m+i+3)(m+i+1)(n+j+1)(n+j-1)}+ \\
&\frac{(n-1)(j-1)(i+m+2)}{(m+i+5)(m+i+3)(n+j+1)(n+j-1)(n+j-3)}- \\
&\frac{(m+1)(j-1)+(i+1)(n-1)}{(m+i+5)(m+i+3)(j+n+1)(j+n-1)}\Bigg]- \\
&\frac{hm^2\gamma m^2}{Dg}\,\frac{a^{m+i+3}}{m+i+3}\left[\frac{b^{n+j-1}-(-b)^{n+j-1}}{n+j-1}\right]\Bigg\}+ \\
&\gamma a^{i+1}\left[b^{j-1}-(-b)^{j-1}\right]=0
\end{aligned}
\tag{25}
$$

DECLASSIFIED

Analysis of torsional deflections.- The thermal buckling which occurred when the longitudinal edges of the cantilever plate were heated resulted in torsional deformations which were similar to the deformations that took place when a constant torque was applied to the plate tip. It was also noted that of the first two modes of vibration, both of which experienced a reduction in natural frequency, the first torsion mode underwent the largest change. Therefore, the remainder of the analysis has been restricted to torsional deformations. Six terms of the deflection function which are antisymmetrical in y have been used. The deflection is then given as

$$\left.\begin{aligned} w = {} & A_{12}x^2y + A_{14}x^2y^3 + \\ & A_{22}x^3y + A_{24}x^3y^3 + \\ & A_{32}x^4y + A_{34}x^4y^3 \end{aligned}\right\} \qquad (26)$$

If the values of m, n, i, and j corresponding to the coefficients of equation (26) are substituted into equation (25), a set of six simultaneous equations is obtained. A matrix of the coefficients of the six equations is symmetrical about the diagonal so that $C_{mn} = C_{nm}$. For a square plate $\frac{a}{b} = 2$ the matrix is

$$\begin{vmatrix} C_{11} & C_{21} & C_{31} & C_{41} & C_{51} & C_{61} \\ C_{21} & C_{22} & C_{32} & C_{42} & C_{52} & C_{62} \\ C_{31} & C_{32} & C_{33} & C_{43} & C_{53} & C_{63} \\ C_{41} & C_{42} & C_{43} & C_{44} & C_{54} & C_{64} \\ C_{51} & C_{52} & C_{53} & C_{54} & C_{55} & C_{65} \\ C_{61} & C_{62} & C_{63} & C_{64} & C_{65} & C_{66} \end{vmatrix} = \begin{vmatrix} C_{17} \\ C_{27} \\ C_{37} \\ C_{47} \\ C_{57} \\ C_{67} \end{vmatrix} \tag{27}$$

where

$$C_{11} = (2.1111 + 0.020318\lambda - 0.016667\beta)a^2$$

$$C_{21} = C_{12} = (0.60555 + 0.0010884\lambda - 0.0025000\beta)a^4$$

$$C_{31} = C_{13} = (2.5000 + 0.016667\lambda - 0.013889\beta)a^3$$

$$C_{41} = C_{14} = (0.65833 + 0.0011905\lambda - 0.0020833\beta)a^5$$

$$C_{51} = C_{15} = (2.8000 + 0.013545\lambda - 0.011905\beta)a^4$$

$$C_{61} = C_{16} = (0.70000 + 0.0010884\lambda - 0.0017857\beta)a^6$$

$$C_{22} = (0.84226 + 0.00036281\lambda - 0.00044643\beta)a^6$$

$$C_{32} = C_{23} = (0.82500 - 0.0020833\beta)a^5$$

$$C_{42} = C_{24} = (0.78839 + 0.00024802\lambda - 0.00037202\beta)a^7$$

$$C_{52} = C_{25} = (1.0333 - 0.00072562\lambda - 0.0017857\beta)a^6$$

$$C_{62} = C_{26} = (0.75429 + 0.00015117\lambda - 0.00031889\beta)a^8$$

$$C_{33} = (3.4000 + 0.015238\lambda - 0.011905\beta)a^4$$

$$C_{43} = C_{34} = (0.95000 + 0.00051422\lambda - 0.0017857\beta)a^6$$

$$C_{53} = C_{35} = (4.1667 + 0.013333\lambda - 0.010417\beta)a^5$$

$$C_{63} = C_{36} = (1.0583 + 0.00071429\lambda - 0.0015625\beta)a^7$$

$$C_{44} = (0.78538 + 0.00022676\lambda - 0.00031888\beta)a^8$$

$$C_{54} = C_{45} = (1.225 - 0.0015625\beta)a^7$$

$$C_{64} = C_{46} = (0.79018 + 0.00017857\lambda - 0.00027902\beta)a^9$$

$$C_{55} = (5.4476 + 0.012314\lambda - 0.0092593\beta)a^6$$

$$C_{65} = C_{56} = (1.4076 + 0.00032983\lambda - 0.0013889\beta)a^8$$

$$C_{66} = (0.82619 + 0.00016491\lambda - 0.00021802)a^{10}$$

$$C_{17} = -\eta$$

$$C_{27} = -\frac{a^2\eta}{4}$$

$$C_{37} = -a\eta$$

$$C_{47} = -\frac{a^3\eta}{4}$$

$$C_{57} = -a^2\eta$$

$$C_{67} = -\frac{a^4\eta}{4}$$

The temperature, frequency, and load parameters, λ, β, and η are defined as

$$\lambda = \frac{a^8 \alpha E a \Delta T}{D} \tag{28}$$

$$\beta = \frac{bm^2 a^4 \gamma \omega^2}{Dg} \tag{29}$$

$$\eta = \frac{2Fb}{D} \tag{30}$$

Related values of temperature, frequency, and deflection under load are obtained by solving the matrix, equation (27). In this analysis, the matrix equation was solved by the Crout method because of its suitability for use with automatic calculating machines. (See ref. 10.)

When there is no vibration or external load, ω and F are zero and the solution of equation (27) gives the temperature difference necessary to produce thermal buckling. For a square plate $\left(\frac{a}{b} = 2\right)$ this difference is

$$\Delta T_{cr} = -\frac{19.98D}{a^2 t K E \alpha} \tag{31}$$

When the value of K given by equation (14) is used, equation (31) becomes

$$\Delta T_{cr} = \frac{18.36D}{a^2 t E \alpha} \; \frac{(\zeta + 3)(\zeta + 1)}{\zeta} \tag{32}$$

Since the flexural stiffness D also contains the modulus E, the critical temperature difference depends only on the plate geometry,

the coefficient of thermal expansion, and Poisson's ratio.

For the case of no heating or external load, ΔT and F are zero and the frequency of the first torsion mode may be obtained. When $\frac{a}{b} = 2$ this value is

$$\omega_0 = \frac{4.185}{a^2\pi} \sqrt{\frac{Dg}{\gamma t}} \tag{33}$$

The frequency given by this relationship is slightly higher than that obtained in the experiments. This is due largely to insufficient clamping of the plate root. For the purpose of comparing measured and calculated results, the theoretical plate was assumed to be slightly longer than the actual plate so that the measured and calculated frequencies would be the same at the start of the test.

If no heat is applied and the plate is not vibrating, (ΔT and ω are zero) the angle of tip rotation resulting from a couple of magnitude $2Fb$ produced by applying a concentrated load F at the tips ($a, \pm b$) of a square plate $\left(\frac{a}{b} = 2\right)$ is

$$\theta_0 = 32.18 \frac{2Fb}{D} \tag{34}$$

DECLASSIFIED

Approximate interaction equations.- The deflection modes of the plate for first-torsion-mode vibration, thermal buckling, and applied torques at the tip are all very similar. If these three modes are assumed to be identical, the deflection can then be expressed as a function with only one arbitrary coefficient and simple interaction equations can be obtained directly by minimizing equation (16) with respect to the single coefficient. If the deflection function is expressed in terms of the deflection of the free corner ($x = a$, $y = b$), equation (15) can be written

$$w = \sum_{m=1}^{\infty} \sum_{n=1}^{\infty} A_{mn} x^{m+1} y^{n-1} \frac{A_{mn} a^{m+1} b^{n-1}}{A_{mn} a^{m+1} b^{n-1}} \tag{35}$$

which reduces to

$$w = \sum_{m=1}^{\infty} \sum_{n=1}^{\infty} \frac{w_{a,b}}{a^{m+1} b^{n-1}} x^{m+1} y^{n-1} \tag{36}$$

where $w_{a,b}$ denotes the deflection of the free corner. From equations (17) - (24), it can be seen that U_B will be proportional to $(w_{a,b})^2$, and that U_M is proportional to $\Delta T(w_{a,b})^2$, U_V is proportional to

$(w_{a,b})^2$, and U_L is proportional to $w_{a,b}$. Since the angle of tip rotation θ (as previously defined) is proportional to $w_{a,b}$, let

$$\left.\begin{aligned} U_B &= \theta^2 U_B' \\ U_M &= \Delta T \theta^2 U_M' \\ U_V &= \theta^2 U_V' \\ U_L &= \theta U_L' \end{aligned}\right\} \qquad (37)$$

A simplified energy equation can now be written as

$$\frac{\partial}{\partial\theta}\left(\theta^2 U_B' + \Delta T \theta^2 U_M' - \omega^2\theta^2 U_V' + \theta U_L'\right) = 0 \qquad (38)$$

If there is no heating or external load

$$\frac{\partial}{\partial\theta}\left(\theta^2 U_B' - \omega^2\theta^2 U_V'\right) = 0$$

and

$$\omega_0 = \sqrt{\frac{U_B'}{U_V'}} \qquad (39)$$

DECLASSIFIED

If there is no vibration or external load, equation (38) becomes

$$\frac{\partial}{\partial\theta}\left(\theta^2 U_B' + \Delta T\theta^2 U_M'\right) = 0$$

and the critical buckling-temperature difference is

$$\Delta T_{cr} = -\frac{U_B'}{U_M'} \tag{40}$$

Similarly, if there is no heating or vibration, the angle of tip rotation for a constant couple is

$$\theta_0 = -\frac{U_L'}{2U_B'} \tag{41}$$

When there is no load and heat is applied during vibration, equation (38) becomes

$$\frac{\partial}{\partial\theta}\left(\theta^2 U_B' + \Delta T\theta^2 U_M' - \omega^2\theta^2 U_v'\right) = 0$$

or, solving for ω, this may be written

$$\omega = \sqrt{\frac{U_B'}{U_v'} + \Delta T\,\frac{U_M'}{U_v'}} \tag{42}$$

DECLASSIFIED

By dividing both sides of equation (42) by ω_0 and by using the relations obtained in equations (39) and (40), the ratio of actual frequency to the initial uniform-temperature frequency is

$$\frac{\omega}{\omega_0} = \sqrt{1 - \frac{\Delta T}{\Delta T_{cr}}} \tag{43}$$

When the external load is applied and the plate is heated (but not vibrated), equation (38) reduces to

$$\frac{\partial}{\partial \theta} \; \theta^2 U_B' + \Delta T \theta^2 U_M' + \theta U_L' = 0$$

and

$$\theta = - \frac{U_L'}{2(U_B' + \Delta T U_M')} \tag{44}$$

When equation (44) is divided by θ_0 and the relationships given by equation (40) and (41) are used, the ratio of the angle of tip rotation to the angle at uniform plate temperature is

$$\frac{\theta}{\theta_0} = \frac{1}{1 - \frac{\Delta T}{\Delta T_{cr}}} \tag{45}$$

DECLASSIFIED

The frequency of vibration is proportional to the square root of the torsional stiffness C, and the angle of twist is inversely proportional to the stiffness. Hence, in this simple case, it is apparent from equations (43) and (45) that

$$\frac{C_e}{C} = 1 - \frac{\Delta T}{\Delta T_{cr}} \tag{46}$$

where C is the torsional stiffness of the unstressed plate and C_e is the effective stiffness of the plate when subjected to thermal stresses.

It is of interest to note that a relationship similar to equation (46) exists for a simple beam subjected to an axial load. The ratio of the effective flexural stiffness of the loaded beam to that of the unloaded beam is

$$\frac{(EI)_e}{EI} = 1 - \frac{F}{F_{cr}} \tag{47}$$

where F is the axial load (positive for tension, negative for compression) and F_{cr} is the load necessary to produce column buckling.

<u>Comparison of interaction relations</u>.- To obtain interaction relations from equation (27), values of ΔT (and hence λ) were

substituted into the equation and the corresponding values of ω (when $F = 0$) and the amplitude coefficients, A_{mn}, for a set value of F (when $\omega = 0$) were determined. From the amplitude coefficients, the angle of tip rotation could be found.

A comparison of the frequencies, tip rotations, and torsional stiffness given by the approximate method (which assumes that the mode shapes are identical) and those obtained by solving equation (27) is given in Table I. The values obtained from equations (43), (45), and (46) are denoted by the subscript i and the values obtained from equation (27) by the subscript d. The related values of temperature, frequency, and deflection under load given by the approximate relations are within 2 percent of the values obtained from equation (27). This small difference arises because the mode shapes produced by thermal buckling, torsional vibration, or a tip couple differ slightly, but it indicates that they are all approximately the same.

The relative values of the amplitude coefficients for the various mode shapes considered are given in Table II. These coefficients do not give a good indication of the similarity of the mode shapes, but, by substituting the values given in Table II into equation (26), an equation of the mode shapes is obtained and their similarity can be noted by comparing the deflections given by each mode at various points. In Tables III and IV, the deflection along the tip ($x = a$) and one edge ($y = b$) are tabulated. These tables show the slight variation in the three mode shapes but also indicate their similarity.

DECLASSIFIED

TABLE I

COMPARISON OF INTERACTION RELATIONS

$\frac{\Delta T}{\Delta T_{cr}}$	Frequency		Tip Rotation		Torsional Stiffness		
	$\left(\frac{\omega}{\omega_o}\right)_i$	$\left(\frac{\omega}{\omega_o}\right)_d$	$\left(\frac{\theta}{\theta_o}\right)_i$	$\left(\frac{\theta}{\theta_o}\right)_d$	$\left(\frac{C_e}{C}\right)_i$	$\left(\frac{\omega}{\omega_o}\right)^2_d$	$\left(\frac{\theta_o}{\theta}\right)_d$
0	1.0000	1.0000	1.0000	1.0000	1.0000	1.0000	1.0000
.2	.8944	.9055	1.2500	1.1983	.8000	.8199	.8345
.4	.7746	.7855	1.6667	1.5247	.6000	.6170	.6559
.6	.6325	.6364	2.5000	2.1713	.4000	.4050	.4606
.8	.4472	.4528	5.0000	4.2409	.2000	.2050	.2558
1.0	0	0	∞	∞	0	0	0

DECLASSIFIED

TABLE II

RELATIVE AMPLITUDE COEFFICIENTS

	Thermal buckling	Torsional vibration	Applied tip couple
A_{12}/A_{12}	1.000	1.000	1.000
A_{14}/A_{12}	.003676	-.001778	-.0001925
A_{22}/A_{12}	-.02147	-.06771	-.04263
A_{24}/A_{12}	-.001082	.0002115	.00002034
A_{32}/A_{12}	-.0003960	.001410	.0006699
A_{34}/A_{12}	.00003225	-.000006372	-.0000006115

DECLASSIFIED

TABLE III

DEFLECTION OF TIP, $x = a$

y	w^*		
	Thermal buckling	Torsional vibration	Applied tip couple
0	0	0	0
2	.2092	.2051	.1995
4	.4162	.4082	.3992
6	.6185	.6061	.5991
8	.8139	.8046	.7994
10	1.000	1.000	1.000

TABLE IV

DEFLECTION OF EDGE, $y = b$

x	w^*		
	Thermal buckling	Torsional vibration	Applied tip couple
0	0	0	0
4	.1296	.1574	.07137
8	.3200	.3937	.2093
12	.5742	.6378	.4645
16	.8797	.9005	.7166
20	1.000	1.000	1.000

*Relative deflections based on $w = 1$ at the free corner

DECLASSIFIED

DECLASSIFIED

BEHAVIOR OF A CANTILEVER PLATE SUBJECTED TO RAPID EDGE HEATING

By Louis Frederick Vosteen

ABSTRACT

The temperature distributions encountered in thin solid wings subjected to aerodynamic heating induce thermal stresses that may effectively reduce the stiffness of the wing. The effects of this reduction in stiffness were investigated experimentally by rapidly heating the edges of a cantilever plate. The midplane thermal stresses imposed by the nonuniform temperature distribution caused the plate to buckle torsionally, increased the deformations of the plate under a constant applied torque, and reduced the frequency of the first bending and first torsion modes of vibration. By using small-deflection theory and employing energy methods, the effect of nonuniform heating on the plate stiffness was calculated. The theory predicts the general effects of the thermal stresses, but becomes inadequate as the edge-to-center temperature difference increases and plate deflections become large.

DECLASSIFIED